# Supporting Information

# Improved photovoltaic performance and stability of quantum dot sensitized solar cells using Mn-ZnSe shell structure with enhanced light absorption and recombination control

Chandu V.V.M. Gopi, M.Venkata-Haritha, Soo-Kyoung Kim, Hee-Je Kim*

*School of Electrical Engineering, Pusan National University, Gumjeong-Ku, Jangjeong-Dong, Busan 609-735, South Korea*

*Corresponding authors. Tel.: +82 51 510 2364; fax: +82 51 513 0212.

E-mail addresses: heeje@pusan.ac.kr (H.-J. Kim).

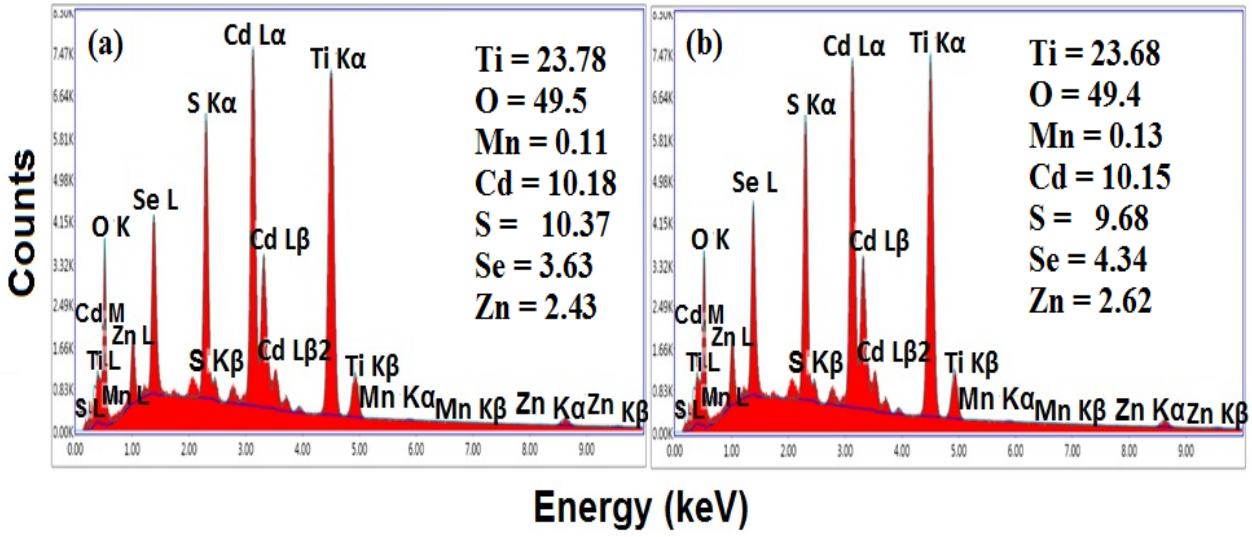


**Figure S1** Energy dispersive X-ray spectroscopy of as-synthesized (a) CdS-CdSe-Mn-ZnS, (b) CdS-CdSe-Mn-ZnSe on the surface of $TiO_2$

EDX analysis was used to clarify the presence of Cd, S, Se, Zn and Mn on the $TiO_2$, as shown in Fig. S1. In CdS-CdSe-Mn-ZnS, the atomic percentages of Cd, S, Se, Zn and Mn were found to be 10.18%, 10.37%, 3.63%, 2.43% and 0.11%, respectively (Fig. 3(a)). Fig. 3(b) shows the EDX analysis of CdS-CdSe-Mn-ZnSe. The percentages of Cd, S, Se, Zn and Mn were obtained as 10.15%, 9.68%, 4.34%, 2.62% and 0.13%, respectively. The elemental Se and Mn content of CdS-CdSe-Mn-ZnSe QDs were substantially higher than that of CdS-CdSe-Mn-ZnS QDs. This was attributed that the ZnSe passivation layer is more favorable for the deposition of metal ions than the ZnS passivation layer. Therefore EDX analysis confirms that the Mn doped passivation layer is successfully deposited on the surface of QDs. In Fig. S1, the energy levels of Mn at 0.650 KeV, 5.89 KeV, and 6.536 KeV correspond to $L_{I\alpha\beta}$, $K_{\alpha}$, and $K_{\alpha\beta}$, respectively.

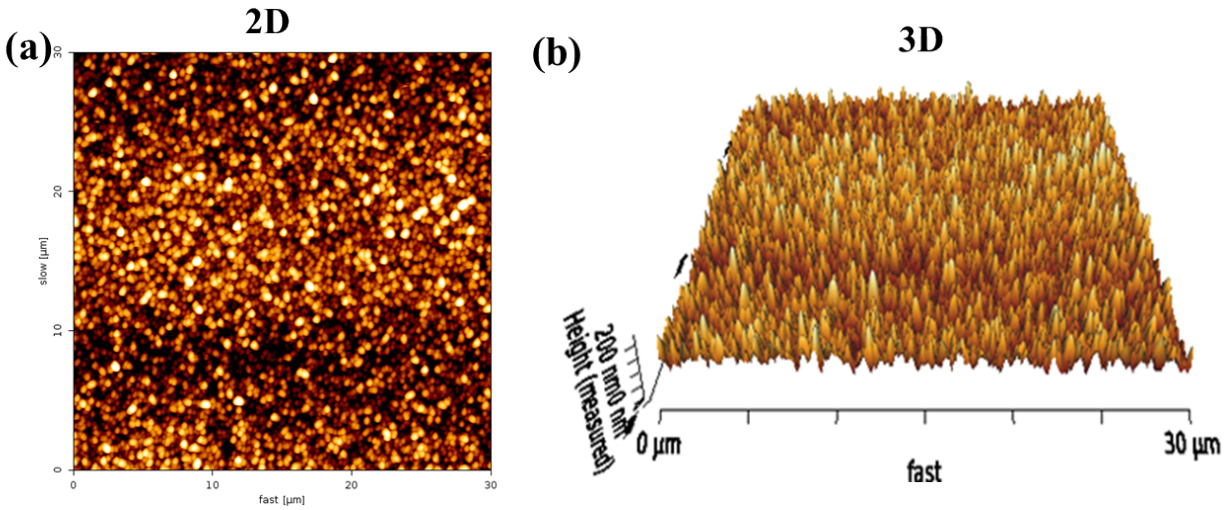


**Figure S2** (a) 2-dimensional (2D) and (b) 3-dimensional (3D) AFM image of FTO-$TiO_2$

The typical root-mean square roughness ($R_q$) was 35.21 nm at deposition of $TiO_2$ on the surface of FTO.

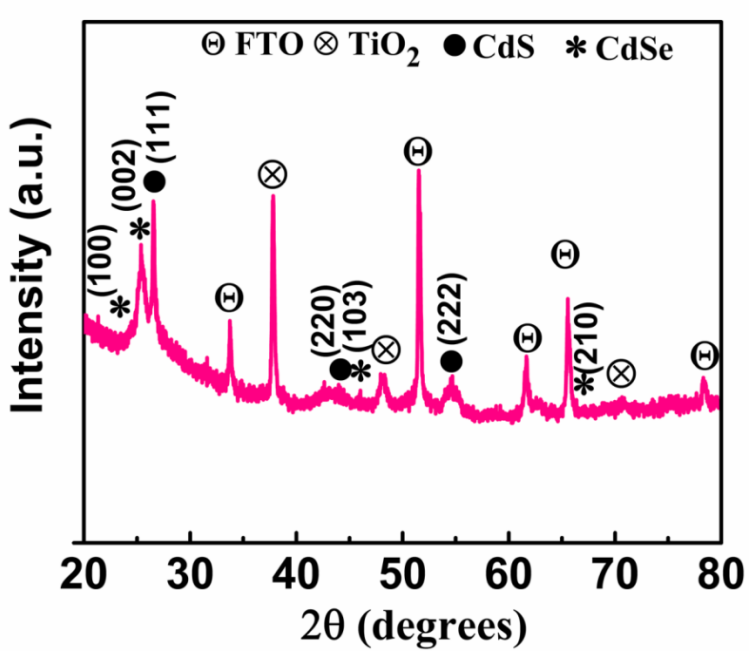


**Figure S3** XRD pattern of CdS-CdSe on the surface of $TiO_2$

The crystallinity of the CdS-CdSe on $TiO_2$ substrate was determined by XRD. As shown in Figure S3, the diffraction peaks are indexed as $TiO_2$ and reveal that the $TiO_2$ nanoparticles have a tetragonal anatase structure (JCPDS: 00-021-1272). As shown in the figure, the peaks that occurred at 26.5, 44.0, and 54.5$^o$ can be indexed to the (111), (220), and (222) planes, similar to the cubic phase facets of CdS (JCPDS: 01-080-0019). Other peaks obtained at 23.7, 25.3, 45.7, and 66.4$^o$ can be assigned to the (100), (002), (103), and (210) facets of the CdSe hexagonal phase (JCPDS: 01-077-2307), respectively. This indicates that CdS and CdSe were successfully deposited on the surface of $TiO_2$.

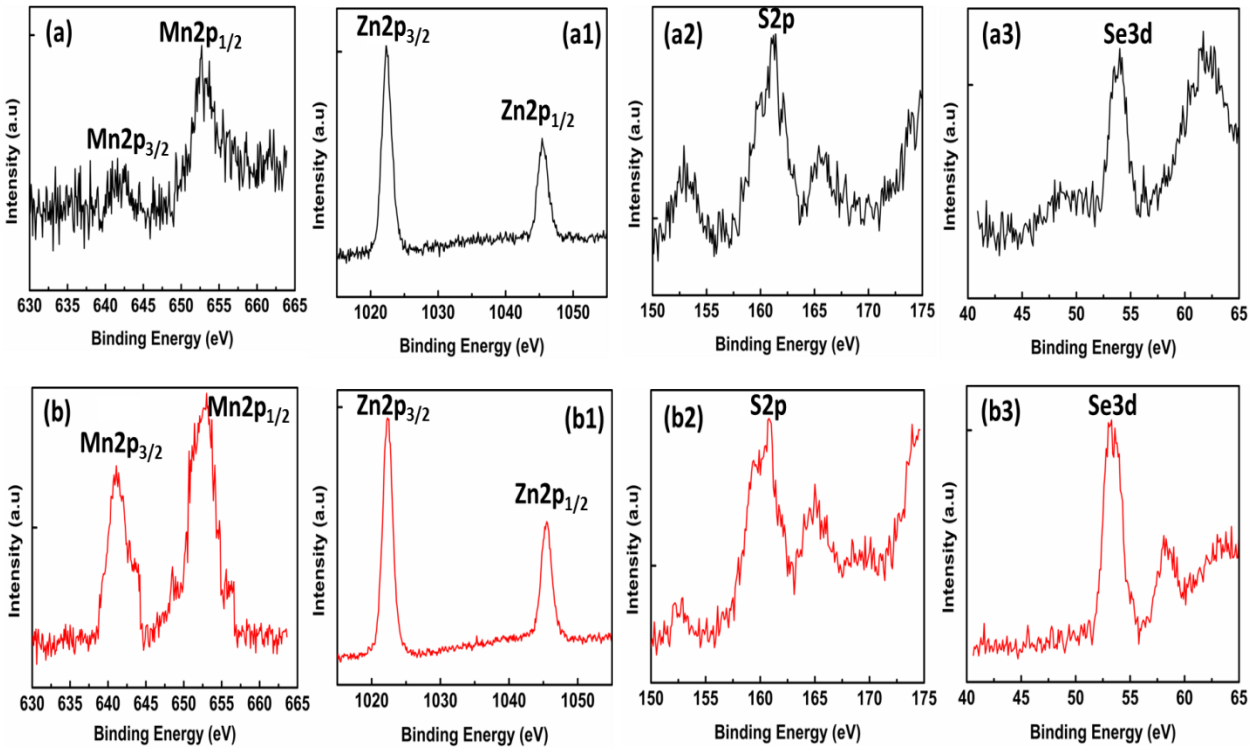


**Figure S4** XPS spectra of Mn-ZnS and Mn-ZnSe on the surface of CdS-CdSe-ZnS

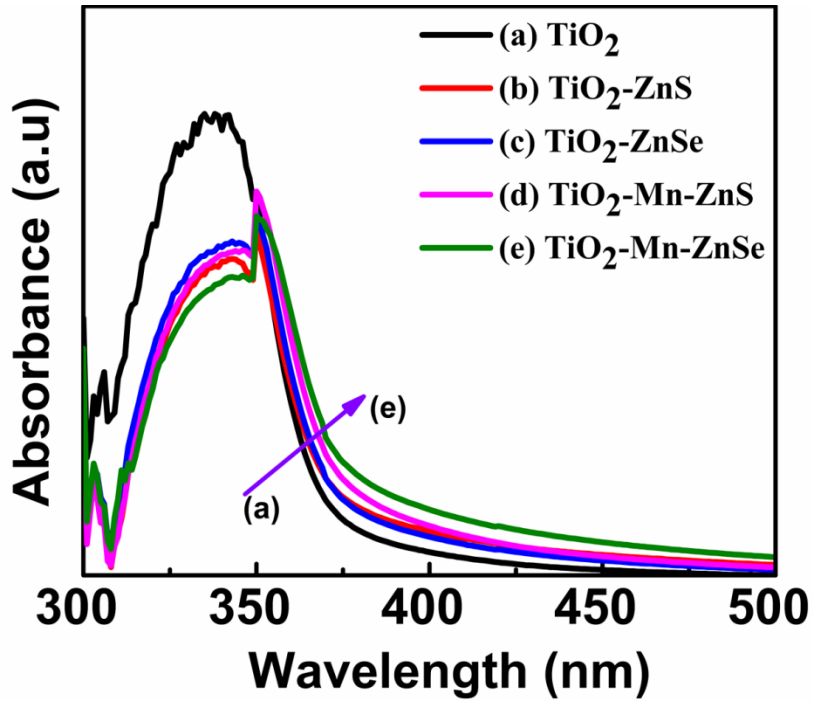


**Figure S5** UV- vis absorption spectra of bare $TiO_2$, $TiO_2$-ZnS, $TiO_2$-ZnSe, $TiO_2$-Mn-ZnS and $TiO_2$-Mn-ZnSe.

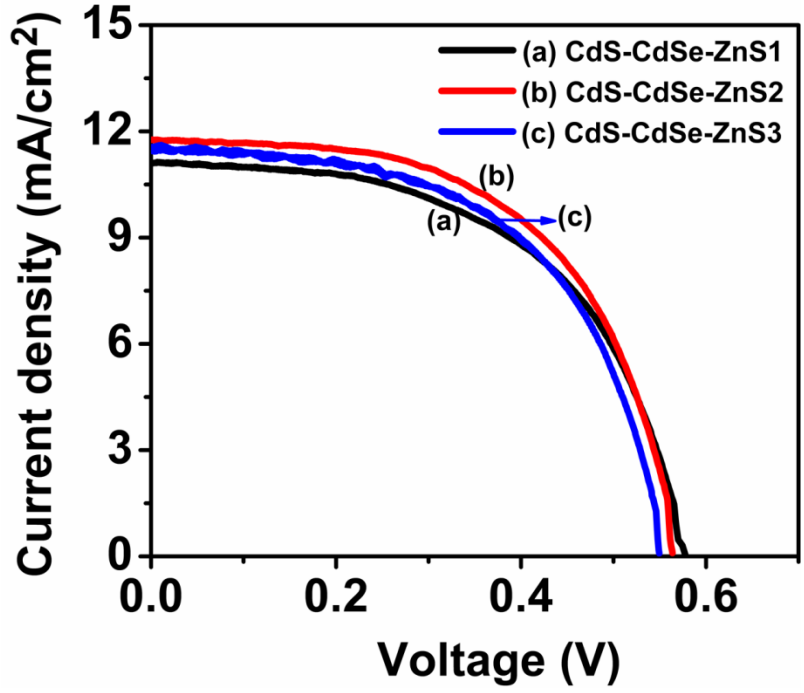

**Figure S6** Power conversion efficiency optimization using J-V curves based on CdS-CdSe with CuS counter electrode and polysulfide electrolyte.

**Table S1** photovoltaic parameters of QDSSCs made with different ZnS SILAR cycles on CdS-CdSe

| Cell | $V_{oc}$ (V) | Jsc(mA/cm$^2$) | FF | η% |
|---|---|---|---|---|
| ZnS1 | 0.577 | 11.13 | 0.550 | 3.54 |
| ZnS2 | 0.565 | 11.75 | 0.575 | 3.82 |
| ZnS3 | 0.549 | 11.61 | 0.564 | 3.59 |

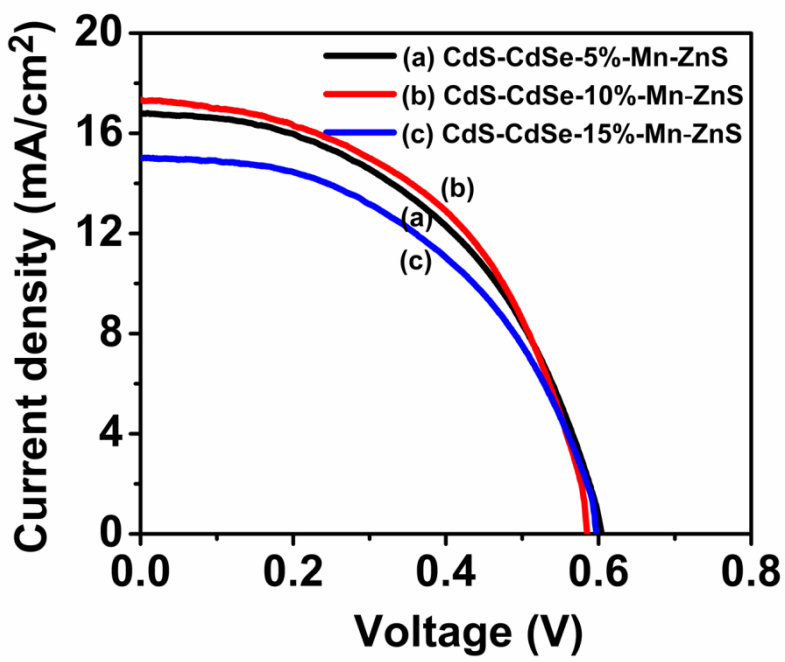


**Figure S7** J–V curves of TiO-Mn-CdS-Cdse-ZnSe based QDSSCs with different ZnSe SILAR post-treatments.]

**Table S2** photovoltaic parameters of QDSSCs made with different doping amount of Mn in ZnS

| Cell | $V_{oc}$ (V) | Jsc(mA/cm$^2$) | FF | η% |
|---|---|---|---|---|
| 5%Mn-ZnS | 0.603 | 16.80 | 0.485 | 4.92 |
| 10%Mn-ZnS | 0.584 | 17.34 | 0.509 | 5.17 |
| 15%Mn-ZnS | 0.596 | 15.02 | 0.492 | 4.41 |